SIMULATION STUDIES OF COLLISION CASCADES IN LIQUID In TARGETS[+]

D.Y. LO[1], M.H. SHAPIRO[2], T.A. TOMBRELLO[1], B.J. GARRISON[3] AND N. WINOGRAD[3]
[1]Division of Physics, Mathematics and Astronomy, Caltech, Pasadena, CA 91125, U.S.A.
[2]Physics Dept., California State University, Fullerton, CA 92634, U.S.A. and Division of Physics, Mathematics and Astronomy, Caltech, Pasadena, CA 91125, U.S.A.
[3]Chemistry Dept., Pennsylvania State University, University Park, PA 16802, U.S.A.

ABSTRACT

Multiple interaction computer simulations have been used to determine the properties of collision cascades in liquid In targets induced by normally incident 5 keV Ar^+ ions. Below the first atomic layer the cascade becomes Thompson-like relatively quickly. However, within the first atomic layer the angular distribution of moving atoms became forward peaked by 150 fs and remained so until ~300 fs. Energy and angle resolved (EARN) spectra were calculated for the ejected atoms. The peak of the energy distribution shifted to lower energies at larger ejection angles, and the angular distributions became broader for lower energy particles. Both results agree with recent experimental data, and with a simple model proposed by Garrison. Our results suggest that the detailed structure of the surface layer is very important in the sputtering process.

INTRODUCTION

In Thompson's model of sputtering [1] the distribution of ejected atoms is given by

$$\frac{d^2N(E,\theta)}{dEd\Omega} = \frac{AE\cos\theta}{(E + U)^{n+1}}. \tag{1}$$

where n depends on the atomic cross section and the nature of the collision cascade inside the target, U is the energy cost [2] to remove an atom from the surface, and A is a normalization constant. Deviations from the pure $\cos\theta$ dependence have been observed in previous experiments and simulations [3,4].

Energy distributions are well described by (1) if U and n are considered free parameters, although U is close to the cohesive energy and n is near 2. The energy and polar angle dependencies are decoupled completely in (1). However, recent energy and angle resolved neutral atom (EARN) spectra of ejected atoms show a shift towards lower energy for the peak in the energy distribution as the polar angle becomes more grazing, and a broadening of the polar angle distribution with decreasing energy [5].

Garrison [6] has proposed a modified version of (1) to fit the EARN data, namely:

$$\frac{d^2N(E,\theta)}{dEd\Omega} = \frac{AE\cos\theta}{(E + U)^{m/2+n+1}} \{U + E\cos^2\theta\}^{m/2}. \tag{2}$$

This formula with its additional free parameter m adequately predicts both the peak position shift in the energy distribution and polar angular distribution broadening. The parameters m and n depend on the nature of the collision cascade inside the target. (1) results from Thomson's assumption of an isotropic velocity distribution inside the target, while Garrison made the *ad hoc* assumption of a $\cos^m\theta$ velocity distribution within the target.

Our simulation studies are aimed at determining the nature of the velocity distribution within a liquid In target. However, on the time scale for the development of a collision cascade (a few hundred femtoseconds) the target can be considered an amorphous solid. Thus, our results should be comparable to those from polycrystalline targets.

The decoupling of angle and energy variables in (1) results from the assumption of an isotropic flux

$$\phi_i(E_i,\theta_i)dE_id\Omega_i \propto \frac{1}{E_i^n} \frac{dE_id\Omega_i}{4\pi} \tag{3}$$

inside the target. (The subscript i denotes variables inside the target.) To obtain the distribution of ejected atoms, the flux perpendicular to the surface is taken and subjected to the variable transformation $E_i \to E$ and $\theta_i \to \theta$ where E and θ are the energy and polar angle measured outside the range of a planar surface potential. Equation (1) then is obtained from

$$\frac{d^2N}{dEd\Omega} = \phi_i(E_i,\theta_i)\cos\theta_i\frac{dE_id\Omega_i}{dE d\Omega}dEd\Omega, \tag{4}$$

with $\phi_i(E_i,\theta_i)$ as given by (3). Garrison assumed an anisotropic flux [6]

$$\phi_i(E_i,\theta_i)dE_i d\Omega_i \propto \frac{\cos^m \theta_i}{E_i^n} dE_i d\Omega_i. \tag{5}$$

Since E_i and θ_i are still decoupled equation (2) can be obtained from (4).

The energy distribution integrated over the hemisphere then is

$$\frac{dN(E)}{dE} = \frac{\pi A}{b} \frac{1}{(E+U)^a} \{(U+E)^b - U^b\}, \tag{6}$$

where $a = (m/2)+n+1$ and $b = (m/2)+1$. This energy distribution has a single peak at $E_p = U\{(a/n)^{1/b} - 1\}$. Careful examination of (2) reveals that while the peak position in the energy distribution for a particular angle depends on n and is proportional to E, the separation between energy peak positions for different angles depends strongly on m. Peak positions generally decrease with n and their separations generally increase with m.

SIMULATION MODEL

The multiple interaction (MI) code SPUT1 [7] was used for this study. Liquid targets consisting of 603 In atoms melted from a fcc structure and heated to a temperature of ~900 K [8] were bombarded with normally incident 5 keV Ar ions. Different liquid targets were generated by modeling the In target without the ion beam present. Atom velocities and positions were stored every picosecond, and the resulting target was used for 25 ion impacts at different locations. Each target was restored to its initial state before each impact in order to simulate the experimental conditions in [5] where the dose was very low. A total of 1000 impacts on 40 different targets were computed on the California State University Cyber-760 computer system.

Pair-wise additive potentials were assumed in the study. The atom-atom potential consisted of a Moliere core joined to a Morse well with a cubic spline. The ion-atom potential was a simple Moliere. Potential parameters were obtained by standard procedures [9-11]. The form of the potentials and the associated parameters are given in Table 1.

Table 1
Potential Parameters

Ion-atom

$$V_{ij} = (A/r)[0.35e^{-0.3r/B} + 0.55e^{-1.2r/B} + 0.1e^{-6r/B}] \qquad r < r_a$$
$$V_{ij} = 0 \qquad r \ge r_a$$
$$A = 12701. \text{ eV·Å} \quad B = 0.09335\,\text{Å} \quad r_a = 2.868\,\text{Å}$$

Atom-atom

$$V_{ij} = (A/r)[0.35e^{-0.3r/B} + 0.55e^{-1.2r/B} + 0.1e^{-6r/B}] \qquad r < r_a$$
$$V_{ij} = C_0 + C_1 r + C_2 r^2 + C_3 r^3 \qquad r_a \le r < r_b$$
$$V_{ij} = D_e[e^{-2b(r-r_e)} - 2e^{-b(r-r_e)}] \qquad r_b \le r < r_c$$
$$V_{ij} = 0 \qquad r \ge r_c$$
$$A = 34574.\,\text{eV·Å} \quad B = 0.08065\,\text{Å} \quad C_0 = 89.151\,\text{eV} \quad C_1 = -23.619\,\text{eV/Å} \quad C_2 = -33.167\,\text{eV/Å}^2$$
$$C_3 = 11.797\,\text{eV/Å}^3 \quad D_e = 0.343\,\text{eV} \quad b = 1.014\,\text{Å}^{-1} \quad r_e = 3.447\,\text{Å} \quad r_a = 1.88\,\text{Å} \quad r_b = 2.04\,\text{Å}$$
$$r_c = 4.71\,\text{Å}$$

- •   0 to 30 degrees
- ▫   30 to 60 degrees   } Simulation
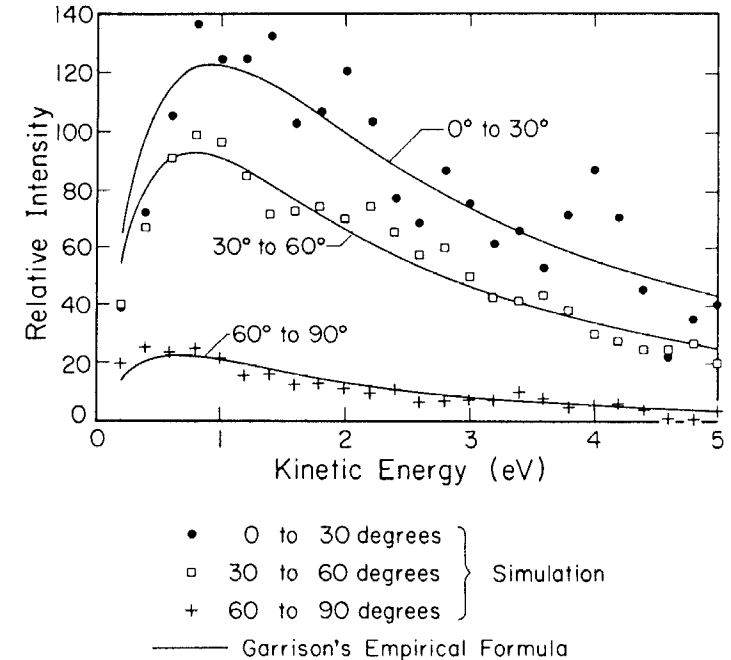- +   60 to 90 degrees
- ——— Garrison's Empirical Formula

Fig. 1 Angle Resolved Energy Spectra

RESULTS

Energy and polar angular distributions of ejected atoms were angle and energy resolved, respectively. Energy distributions were obtained for angular intervals of 0° to 30°, 30° to 60°, and 60° to 90°. Polar angular distributions were obtained for energy intervals of 0 to 2 eV, 2 to 4 eV, and 4 to 6 eV (figs. 1 and 2). The peak positions of the energy distributions clearly exhibit a shift toward higher energies
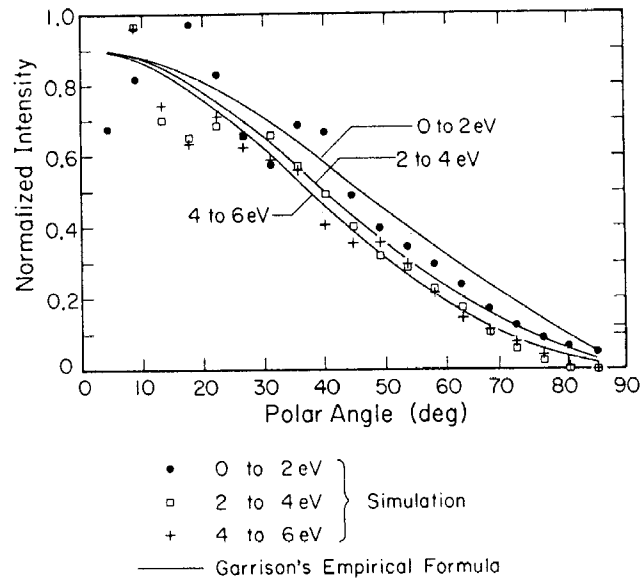

Fig. 2 Energy Resolved Angular Distributions

with decreasing polar angles, while the polar angular distributions broaden with lower energies. These trends basically agree with the experimental EARN data [5] and the predictions of Garrison [6]. The distributions predicted by (2) with m = 2.22, n = 2.07, and U = 1.98 eV are shown in figs. 1 and 2 for comparison. The parameters m, n, and U were obtained by fitting the simulated angle-integrated energy distributions to (6). This resulted in a simulated angle-integrated energy distribution peak at 0.8 eV in comparison to the experimentally observed value of ~2 eV [5].

The energy and polar angular distributions of atoms with kinetic energy > 1 eV in the first and second surface layers of the target were sampled at various

times throughout the collision cascade. The 1 eV cut-off excluded most of the atoms outside the collision cascade. The first layer distributions were fitted to the anisotropic flux of (3) which was assumed by Garrison. Since $d^2N_i/dE_i d\Omega_i$ = $(2mE_i)^{-1/2} \Phi_i(E_i,\theta_i)$, dN_i/dE_i was fitted to $A/E^{n+1/2}$ while $dN_i/d\Omega_i$ was fitted to $B\cos^m\theta + C$ where A, B, and C are constants. The finite bin size of the simulated distributions was accounted for by integrating the analytical expressions over each bin before fitting. All fitting was done by minimizing χ^2 assuming that the uncertainty in the simulated distributions was governed by a Poisson distribution. The resulting values of m and n are tabulated in Table 2. The small values of χ^2_ν are an indication that Poisson statistics overestimates the uncertainties in the simulated spectra.

Table 2

First Layer Flux Distribution Parameters

Time (fs)	m	χ^2_ν	n	χ^2_ν
100	0.52 (.25)*	0.38	0.67 (.17)*	0.47
150	1.4 (.65)	0.38	0.75 (.10)	0.42
200	1.1 (.27)	0.30	1.0 (.10)	2.2
250	1.5 (.42)	0.65	1.4 (.10)	3.8
300	1.1 (.35)	0.63	1.8 (.12)	2.3
400	0.46 (.22)	0.56	2.4 (.21)	1.8

*The quantities in parenthesis are the expected statistical uncertainties assuming a Poisson distribution.

The first layer angular distribution shows a definite forward peak by 150 fs and becomes nearly isotropic by 400 fs (Table 2 and fig. 3). The greatest anisotropy occurs at ~250 fs. This should be the most important distribution since all sputtered atoms must traverse the first layer, and most atoms are ejected near this time in the cascade development. The second layer angular distribution is isotropic from 100 to 300 fs, then becomes transversely peaked by 400 fs. This may be an artifact of the finite size and slab-like geometry of the target. The energy distribution parameter n increases monotonically with time and has roughly the same value for the first and second atomic layers. This reflects the steady degradation in average energy of the atoms as the collision cascade ages.

DISCUSSION

Our results show that the presence of a free surface (neglected in the Thompson model) causes significant anisotropy in the first layer flux. This
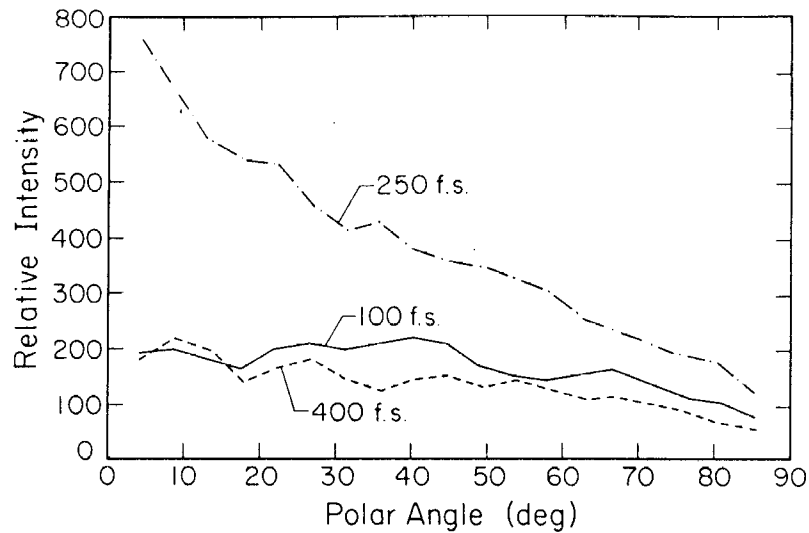
Fig. 3 Time Development of First Layer Angular Distributions

anisotropy diminishes quickly in the subsurface layers. The strong anisotropy in the surface layer portion of the collision cascade occurs at the time when the greatest number of atoms are ejecting. This has significant effects on the sputtered atom distributions. These effects have been seen both in recent experiments and the present simulations.

It is clear from our simulation that both the peak position shift in the energy distribution and the broadening of the angular distributions can be explained using pairwise interactions of the target atoms. However, the large discrepency between the energy peak position in the simulated spectra (0.8 eV), and the experimental value (~2 eV) may reflect some inadequacy in the pair potential model. Studies which include many body effects through the use of an effective medium model are now underway [12].

References

1. M.W. Thompson, Phys. Rept. 69, 337 (1981).
2. B.J. Garrison, N. Winograd, D.Y. Lo, T.A. Tombrello, M.H. Shapiro, and D.E. Harrison Jr.,
   Surf. Sci. (1986) in press.
3. M.F. Dumke et al., Surf. Sci. 124, 407 (1983).
4. M.H. Shapiro, D.Y. Lo, P.K. Haff and T.A. Tombrello, NIM B13, 348 (1986).

5. J.P. Baxter, J. Singh, G.A. Schick, P.H. Kobrin, and N. Winograd, NIM B17, 300 (1986).
6. B.J. Garrison, NIM B17, 305 (1986).
7. M.H. Shapiro, Technical Rept. BB-1 Caltech (1983).
8. D.Y. Lo, T.A. Tombrello and M.H. Shapiro, NIM B17, 207 (1986)
9. I.M. Torrens, Interatomic Potentials. (Academic Press, New York, 1972).
10. L.A. Girifalco and V.G. Weizer, Phys. Rev. 114, 687 (1959).
11. C. Kittel, Introduction to Solid State Physics, 5th ed. (Wiley, N.Y., 1976).
12. B.J. Garrison, N. Winograd, D.Y. Lo, T.A. Tombrello, M.H. Shapiro, and D.E. Harrison, Jr., in preparation.